ELSEVIER

Journal of Alloys and Compounds 227 (1995) 5–9

Journal of ALLOYS AND COMPOUNDS

Enhanced oxidation of nickel in atomic oxygen

S.A. Raspopov [a], A.G. Gusakov [a], A.G. Voropayev [a], A.A. Vecher [a], V.K. Grishin [b]

[a] *Chemical Department, Belarus State University, Skorina Avenue 4, Minsk 220050, Belarus*

[b] *Russian Rockets and Space Corporation "Energija", Kaliningrad, 141070 Moscow Oblast, Russia*

Received 10 December 1994

Abstract

The oxidation of nickel in atomic oxygen has been investigated at the conditions close to those of a low Earth orbit (at an atomic oxygen incident flux of 10^{16}–6×10^{16} atoms cm^{-2} s^{-1}) and in the temperature range 773–1373 K. The rate constant of nickel oxidation in atomic oxygen at low pressures was found to be higher by orders of magnitude than that in diatomic oxygen having the same pressure even at these rather high temperatures. As regards the dependence of oxidation rate on oxygen pressure, while in diatomic oxygen the parabolic rate constant of nickel oxidation is proportional to $P_{O_2}{}^{0.35}$, in atomic oxygen it is proportional to $P_O{}^{0.72}$ (the power is twice that in O_2). Also, the activation energy of oxidation decreases from 182 kJ mol^{-1} for molecular oxygen to 76 kJ mol^{-1} for atomic oxygen. A model is proposed explaining these observations, which is based on the assumption that atomic oxygen in the gas phase and the oxygen chemisorbed on the NiO surface are close to equilibrium.

Keywords: Nickel, Oxidation; Atomic oxygen; Low pressures

1. Introduction

The kinetics of nickel interaction with atomic oxygen have not so far been investigated. It was revealed in experiments on the Space Shuttle that the oxidation of nickel in atomic oxygen takes place even at ambient temperatures (225–300 K) [1–3]. It was reported in [4] that the oxidation rates of Ni, Zr, Mo and Ta at 773–963 K do not increase in the presence of atomic oxygen (in comparison with diatomic oxygen); only for copper a considerable effect was observed. However, these experiments were carried out at a very low oxygen dissociation efficiency (about 0.1%) and at higher pressures (50–500 Pa). In our previous work [5] a strong build-up of Ta oxidation rate in atomic oxygen was revealed at an oxygen pressure of 10^{-2}–0.1 Pa and at temperatures above 773 K. In [6] no enhancement of Ni, Armco iron and stainless steel oxidation owing to atomic oxygen was observed as well (at 1400–1600 K), but these experiments were conducted at an even higher pressure (1.5 MPa). Thermal decomposition of N_2O was used to obtain atomic oxygen in this work, which enters immediately into the subsequent reactions in gas phase. Nickel oxidation in diatomic oxygen has been investigated by many researchers [7–10]. Parabolic oxidation was observed at temperatures above 800 K. The rate of oxidation is determined by the diffusion of Ni ions via a scale. The oxidation activation energy (about 185 kJ mol^{-1}) agrees well with the activation energy of nickel ion diffusion in NiO (189 kJ mol^{-1} [11]). The present research has been conducted with an incident oxygen atom flux in the range from 10^{16} to 6×10^{16} atoms cm^{-2} s^{-1}, i.e. under conditions close to those of a low Earth orbit and at temperatures between 773 and 1373 K.

2. Experimental details

The experimental methods have been described in more detail in our recent publications on the oxidation of group VB metals in atomic oxygen [5,12,13]. The apparatus consists of a vacuum system with a quartz reaction chamber which is coupled to a 600 l s^{-1} diffusion pump. The flow of gas mixture to the reaction chamber was fixed by the needle valve at a rate of 2–7 cm^3 (STP) min^{-1}. The specimen was placed in the reaction chamber; the oxygen pressure at the location of the specimen was 10^{-2}–10^{-1} Pa. The gas mixture was passed through a 2400 MHz, 60 W microwave discharge cavity before entering the reaction chamber so that atomic oxygen was obtained. NO_2 chemiluminescent titration was used to determine the oxygen dissociation efficiency. We use oxygen–nitrogen gas mixtures as a rule; this enables us to vary the oxygen dissociation efficiency from 4.5 to 45% by

0925-8388/95/$09.50 © 1995 Elsevier Science S.A. All rights reserved
SSDI 0925-8388(95)01643-0

varying the composition of the mixture. Also, experiments with oxygen–argon mixtures were carried out, which well confirmed the kinetic data obtained using O_2–N_2 mixtures.

Our specimens were nickel ribbons 1.5 mm × 0.05 mm in cross-section. They were annealed in a high vacuum at 1473 K for 4 h. The main impurities were 1000 ppm Mg, 100 ppm Cu and Zn and 10 ppm Mn and Pb. The technique used to study the kinetics of oxidation was to monitor continuously the electrical resistance–time curve of a resistively heated specimen. Together with the electrical current measurements, the voltage drop across the central 1.5 cm of a ribbon was measured using nickel contacts, welded to the specimen. The specimen was maintained at a constant temperature by altering an a.c. in accordance with a chromel–alumel thermocouple (welded to the centre of the specimen) output. Thermocouple readings were corrected for the heat removal via thermocouple wires. This was done by the comparison of the electrical resistance–temperature relationships obtained when the specimen was heated resistively and in the furnace (in a high vacuum). The correction increases with increasing temperature but it does not exceed 20 K.

The results of experiments are presented as the ratio (R/R_0) of the current value of resistance of the central part of the specimen to that before the beginning of oxidation, but at the temperature of experiment in order to avoid errors associated with a possible change in distance between the welded contacts. This method has demonstrated good reproducibility of kinetic data in our previous work [5,12,13]; for nickel, good reproducibility was observed as well. The parabolic rate constants obtained in several experiments under similar conditions never differed by more than 20%. Metallographic studies showed that the thickness of the metallic core of the oxidized specimens values by the end of the experiment agree well with those calculated from the data on electrical resistance.

Experiments in low pressure (about 10^{-2} Pa) diatomic oxygen showed that at 1273 K the parabolic rate constant of nickel oxidation is a tenth of that in atomic oxygen at the same pressure. At lower temperatures the oxidation rate is too low to record reliably by the resistance measurements at all. Thus all the observed rate of nickel oxidation in dissociated oxygen (28.7% is the typical dissociation efficiency value) can be attributed to atomic oxygen. This helps the interpretation of results.

Since it was reported [14] that UV radiation strongly accelerates the oxidation of nickel in molecular oxygen, a number of experiments have been carried out in which the specimen was hidden by a shield from the UV radiation emanating from microwave discharge. However, in our experiments (when oxidation occurs in atomic oxygen), no marked difference was found between oxidation rates when the specimen is hidden and when it is not.

3. Results

As X-ray diffraction studies demonstrated, NiO was the only oxide formed in all our experimental conditions. The

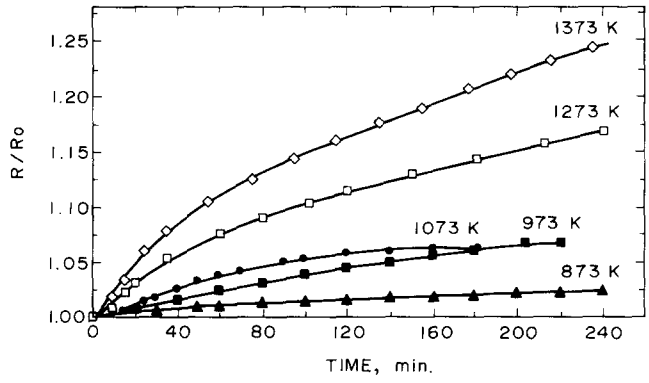

Fig. 1. Electrical resistance vs. time plot for oxidation of nickel in atomic oxygen at an incident flux of 2.7×10^{16} atoms cm^{-2} s^{-1} and at different temperatures.

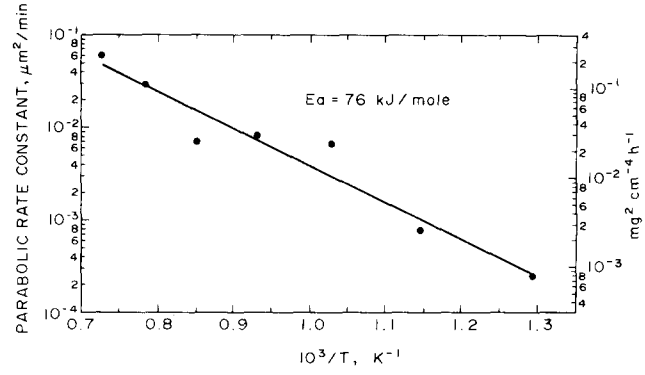

Fig. 2. Arrhenius plot of the parabolic rate constant of nickel oxidation at an atomic oxygen incident flux of 2.7×10^{16} atoms cm^{-2} s^{-1}.

kinetic curves of nickel oxidation at an atomic incident flux of 2.7×10^{16} atoms cm^{-2} s^{-1} at different temperatures are presented in Fig. 1. These data were obtained at an oxygen dissociation efficiency of 28.7%, when air is passed through the microwave discharge cavity. The kinetic curves correspond to parabolic oxidation, i.e.

$$\frac{dS}{dt} = \frac{4K_p}{S-S_0} \quad (1)$$

where K_p is the parabolic rate constant of oxidation, S is the metallic core of specimen thickness current value and S_0 is the initial thickness of a ribbon. The factor 4 in the right-hand part of Eq. (1) takes into account the fact that oxidation occurs at both ribbon surfaces.

Fig. 2 gives the temperature dependence of the parabolic rate constant, calculated from the data shown in Fig. 1. The values on the right-hand vertical axis are calculated from the same data, using the known value of nickel density (8.91 g cm^{-3}).

Since oxidation in diatomic oxygen at low pressures was too slow and the kinetics could hardly be studied, experiments at diatomic oxygen pressures up to 1 atm were conducted. No flow was passed through the system in these experiments. The samples resistance vs. time plot for nickel oxidation in

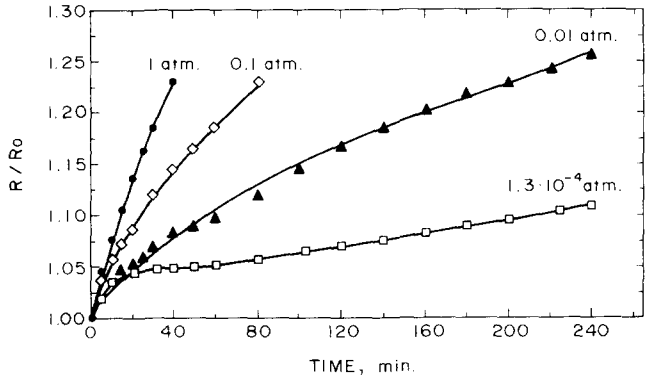

Fig. 3. Kinetic curves of nickel oxidation in air at different pressures and 1273 K.

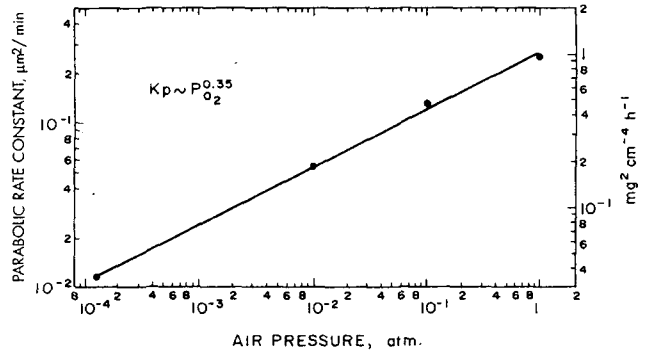

Fig. 4. Parabolic rate constant vs. air pressure plot for oxidation of nickel at 1273 K.

Table 1
Dependence of the parabolic rate constant of nickel oxidation in air at 0.1 atm on temperature

T (K)	K_p (μm^2 min^{-1})
1173	0.0335
1273	0.151
1373	0.505

air at 1273 K and different pressure values is presented in Fig. 3. The dependence of the parabolic rate constant on the air pressure is shown in Fig. 4; K_p is proportional to $P_{O_2}^{0.35}$. Presumably this value of the power indicates that neutral and singly ionized nickel vacancies prevail in NiO[11] under our experimental conditions.

The temperature dependence of the rate of oxidation in diatomic oxygen was studied in air at 0.1 atm. The results are given in Table 1; they correspond to an activation energy of 182 kJ mol^{-1}, which coincides well with the averaged value of 185 kJ mol^{-1}, obtained previously [7–9].

Thus activation energy of nickel oxidation in atomic oxygen ($E_a = 76$ kJ mol^{-1} (Fig. 2)) appears to be much lower than for diatomic oxygen ($E_m = 182$ kJ mol^{-1}).

Fig. 5 gives the resistance as a function of time for nickel oxidation at 1273 K and different atomic oxygen incident flux values and the corresponding K_p vs. atomic oxygen incident flux plot is adduced in Fig. 6.

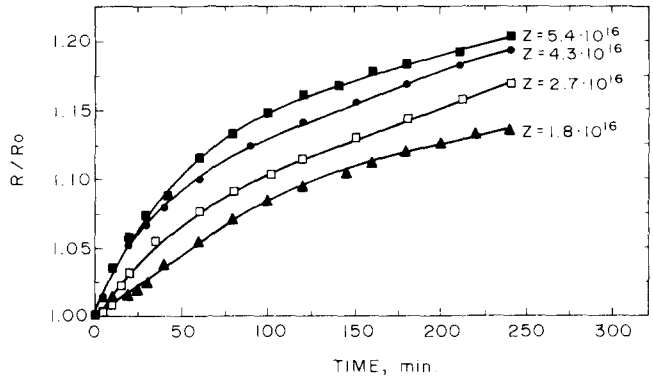

Fig. 5. Kinetic curves of nickel oxidation in atomic oxygen at different values of incident flux Z (atoms cm^{-2} s^{-1}) and 1273 K.

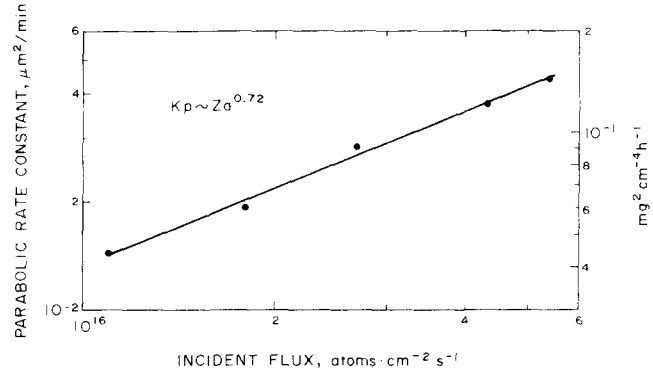

Fig. 6. Parabolic rate constant vs. atomic oxygen incident flux plot for the oxidation of nickel at 1273 K.

The incident flux is proportional to pressure in accordance with the Hertz–Knudsen equation

$$Z = \frac{P}{(2\pi mkT)^{1/2}} \quad (2)$$

where m is the mass of atom or molecule and k is the Boltzmann constant. Consequently, it follows from Figs. 4 and 6 that the dependence of the parabolic rate constant on pressure or incident flux is much stronger for oxidation in atomic oxygen than for oxidation in molecular oxygen (the power for the former is approximately twice that for the latter).

4. Discussion

Since the limiting stage of nickel oxidation at the temperatures under consideration in this paper is the diffusion of nickel ions via a scale, a strong increase in the rate of oxidation in atomic oxygen can arise only because oxygen atoms are chemisorbed on an oxide surface much more easily than are oxygen molecules, thereby increasing strongly the NiO surface coverage of chemisorbed oxygen and the oxygen chemical potential on the oxide surface.

Now let us consider two models of the processes taking place on the NiO surface during the nickel oxidation in diatomic and atomic oxygen. In model 1 the traditional approach is used, but it fails to explain our observations. Model 2 is in much better agreement with our experimental data.

4.2. Model 1

As the nickel oxidation rate is limited by the diffusion in the oxide film, we may assume that the rates of oxygen chemisorption and desorption from the NiO surface are approximately equal. For oxidation in atomic oxygen this can be written as (see Eq. (2))

$$\frac{P_O}{(2\pi mkT)^{1/2}} S_a = 2K_d\theta^2 \tag{3a}$$

where P_O is the pressure of atomic oxygen, m is the mass of oxygen atom, S_a is the chemisorption probability of atomic oxygen on the NiO surface, θ is the fractional surface coverage of chemisorbed oxygen atoms and K_d is the desorption rate constant. For oxidation in diatomic oxygen this condition will be given by

$$\frac{P_{O_2}}{(4\pi mkT)^{1/2}} S_m = K_d\theta^2 \tag{3b}$$

where S_m is the molecular oxygen chemisorption probability.

Now let us introduce a quantity "effective pressure P_{O_2}* of diatomic oxygen". This will be the pressure of diatomic oxygen, which corresponds to the same fractional surface coverage of chemisorbed oxygen (and, consequently, to the same chemical potential of oxygen on the NiO surface) as in atomic oxygen having the pressure P_O. This value can be calculated from Eqs. (3a) and (3b):

$$P_{O_2}{}^* = \frac{P_O S_a}{2^{1/2} S_m} \tag{4}$$

Since the temperature dependences of the chemisorption probabilities can be given by

$$S_a = S_a{}^0 \exp\left(-\frac{E'}{RT}\right)$$

$$S_m = S_m{}^0 \exp\left(-\frac{E''}{RT}\right) \tag{5}$$

where E' and E'' are the activation energies of chemisorption of atomic and diatomic oxygen respectively on the NiO surface, and $S_a{}^0$ and $S_m{}^0$ are the pre-exponential factors, Eq. (4) will have the following form:

$$P_{O_2}{}^* = \frac{P_O S_a{}^0}{2^{1/2} S_m{}^0} \exp\left(\frac{E''-E'}{RT}\right) \tag{6}$$

The dependence of the parabolic rate constant on the temperature and molecular oxygen pressure has the following general form:

$$K_p = K_0 \exp\left(-\frac{E_m}{RT}\right) P_{O_2}{}^n \tag{7}$$

where E_m is the activation energy of oxidation in molecular oxygen and K_0 is the pre-exponential factor. K_p is proportional to $P_{O_2}{}^{0.35}$ for oxidation in diatomic oxygen (Fig. 4); consequently, for oxidation in atomic oxygen,

$$K_p = K_0 \exp\left(-\frac{E_m}{RT}\right) (P_{O_2}{}^*)^{0.35} \tag{8}$$

Furthermore, using Eq. (6), we obtain

$$K_p = K_0 \exp\left(\frac{0.35(E''-E') - E_m}{RT}\right)\left(\frac{P_O S_a{}^0}{2^{1/2} S_m{}^0}\right)^{0.35} \tag{9}$$

Thus, according to Eq. (9), K_p is proportional to $P_O{}^{0.35}$, i.e. the power is the same as in the case of diatomic oxygen, but this does not conform with the experimental data (Fig. 6). Also, in accord with Eq. (9), the activation energy of nickel oxidation in atomic oxygen is

$$E_a = E_m - 0.35(E''-E') \tag{10}$$

As $E_a = 76$ kJ mol^{-1} (Fig. 2) and $E_m = 182$ kJ mol^{-1}, consequently $E''-E' = 297$ kJ mol^{-1}. The activation energy of atomic oxygen chemisorption must not be below zero; consequently the activation energy of E'' of chemisorption of molecular oxygen must be 297 kJ mol^{-1} or more; however, this is impossible because the activation energy of the whole process of oxidation in molecular oxygen is 182 kJ mol^{-1} and not oxygen chemisorption; but diffusion in oxide film is the limiting stage of nickel oxidation in diatomic oxygen. Consequently, this model fails to explain such a strong difference between the activation energies of nickel oxidation in atomic and diatomic oxygen (76 kJ mol^{-1} and 182 kJ mol^{-1} respectively). Thus this traditional approach, which we used to explain the features observed for tantalum oxidation in molecular and atomic oxygen at low pressures [5], apparently cannot be used in this case.

4.2. Model 2

Let us suppose that oxygen chemisorbed on the NiO surface and atomic oxygen in the gas phase are in equilibrium during oxidation in atomic oxygen. In this case,

$$P_{O_2}{}^* = P_O{}^2 \exp\left(\frac{\Delta G_d{}^0(T)}{RT}\right) \tag{11}$$

where $\Delta G_d{}^0$ is the standard Gibbs energy of the dissociation of oxygen, i.e. of the reaction $O_2 \rightleftarrows 2O$.

Substituting P_{O_2}* from Eq. (11) into Eq. (8) we have

$$K_p = K_0 \exp\left(\frac{0.35\ \Delta G_d{}^0(T) - E_m}{RT}\right) P_O{}^{0.7} \tag{12}$$

So, K_p is proportional to $P_O{}^{0.7}$, which is in good agreement with the experimental power value of 0.72 (Fig. 6).

The activation energy of oxidation in atomic oxygen can be calculated from Eq. (12) as well:

$$E_a = E_m - 0.35\ \Delta G_d^0(1100\ \text{K}) \quad (13)$$

1100 K is the average temperature of our experiments.

From [15], $\Delta G_d^0(1100\ \text{K}) = 362.7\ \text{kJ mol}^{-1}$; consequently E_a is 54.8 kJ mol^{-1}. This should be considered as in good agreement with the experimental value of 76 kJ mol^{-1}, because it is clear that true equilibrium cannot exist between the chemisorbed oxygen on the NiO surface and atomic oxygen in the gas phase. This would be possible only if recombination of atomic oxygen did not occur on the NiO surface at all, but this condition can hardly be satisfied. For a temperature of 1273 K and $P_0 = 10^{-7}$ atm, $P_{O_2}{}^* \approx 1$ atm (from Eq. (11)); consequently, the rate constant of oxidation in atomic oxygen at 10^{-7} atm (the incident flux is 2.7×10^{16} atoms cm^{-2} s^{-1}) should be equal to that in molecular oxygen at 1 atm in the case of true equilibrium, but it is about a tenth of it (see Figs. 4 and 6). So, true equilibrium is not reached in our experiments; nonetheless, this model explains the data obtained, at least qualitatively.

Acknowledgements

We are grateful to Dr. A.A. Savitski for assistance with the preparation of specimens and to Mr. A.S. Sobeski for the X-ray work. The work was supported by the Ministry of Science and Education of Belarus and by Belarus Space Council.

References

[1] L.J. Leger, B. Santos-Mason, J. Visentine and J. Kuminescz, in D.E. Brunza (ed.), *Proc. NASA Workshop on Atomic Oxygen Effects,* in *Publ. 87-14,* 1987, p. 1 (Jet Propulsion Laboratory, Pasadena, CA).
[2] P.N. Peters, J.C. Gregory and J.T. Swann, *Appl. Opt., 25* (1986) 1290.
[3] J.S. Brodkin, L.C. Sengupta, W. Franzen and P.L. Sagalyn, *Thin Solid Films, 234* (1993) 512.
[4] A. Dravnicks, *J. Am. Chem. Soc., 72* (1950) 3761.
[5] A.G. Gusakov, S.A. Raspopov, A.A. Vecher and A.G. Voropayev, *J. Alloys Comp., 201* (1993) 67.
[6] V.L. Bolobov and K.M. Makarov, *Zashch. Met., 28* (1992) 1007 (in Russian).
[7] O. Kubaschewski and B.E. Hopkins, *Oxidation of Metals and Alloys,* Butterworths, London, 1953.
[8] E. Fromm and E. Gebhardt, *Gases and Carbon in Metals,* Springer, Berlin, 1976.
[9] J. Bernard, *Oxidation of Metals,* Gauthier-Villars, Paris, 1962 (in French).
[10] A. Atkinson and D.W. Smart, *J. Electrochem. Soc., 135* (1988) 2886.
[11] P. Kofstad, *High-Temperature Oxidation of Metals,* Wiley, New York, 1966.
[12] S.A. Raspopov, A.G. Gusakov, A.G. Voropayev and A.A. Vecher, *J. Alloys Comp., 205* (1994) 59.
[13] S.A. Raspopov, A.G. Gusakov, A.G. Voropayev and A.A. Vecher, *J. Alloys Comp., 205* (1994) 191.
[14] A. Mesarwi and A. Ignatiev, *J. Vac. Sci. Technol. A, 7* (1989) 1754.
[15] JANAF Thermochemical Tables, 1982 Supplement, in *J. Phys. Chem., Ref. Data, 1* (3) (1982).